International Journal of Nanomedicine

Dovepress
open access to scientific and medical research

Open Access Full Text Article

ORIGINAL RESEARCH

Electrospun chitosan-graft-poly (ε-caprolactone)/poly (ε-caprolactone) nanofibrous scaffolds for retinal tissue engineering

This article was published in the following Dove Press journal:
International Journal of Nanomedicine
23 February 2011
Number of times this article has been viewed

Honglin Chen[1,2]
Xianqun Fan[1]
Jing Xia[1]
Ping Chen[1]
Xiaojian Zhou[1]
Jin Huang[2]
Jiahui Yu[2]
Ping Gu[1]

[1]Department of Ophthalmology, Shanghai Ninth People's Hospital, School of Medicine, Shanghai Jiaotong University, Shanghai, China; [2]Institutes for Advanced Interdisciplinary Research, East China Normal University, Shanghai, China

Abstract: A promising therapy for retinal diseases is to employ biodegradable scaffolds to deliver retinal progenitor cells (RPCs) for repairing damaged or diseased retinal tissue. In the present study, cationic chitosan-graft-poly(ε-caprolactone)/polycaprolactone (CS-PCL/PCL) hybrid scaffolds were successfully prepared by electrospinning. Characterization of the obtained nanofibrous scaffolds indicated that zeta-potential, fiber diameter, and the content of amino groups on their surface were closely correlated with the amount of CS-PCL in CS-PCL/PCL scaffolds. To assess the cell–scaffold interaction, mice RPCs (mRPCs) were cultured on the electrospun scaffolds for 7 days. In-vitro proliferation assays revealed that mRPCs proliferated faster on the CS-PCL/PCL (20/80) scaffolds than the other electrospun scaffolds. Scanning electron microscopy and the real-time quantitative polymerase chain reaction results showed that mRPCs grown on CS-PCL/PCL (20/80) scaffolds were more likely to differentiate towards retinal neurons than those on PCL scaffolds. Taken together, these results suggest that CS-PCL/PCL(20/80) scaffolds have potential application in retinal tissue engineering.

Keywords: electrospun, retinal progenitor cells, proliferation, differentiation, tissue engineering

Introduction

Retinitis pigmentosa and age-related macular degeneration are two major retinal diseases characterized by the progressive deterioration of the retina, ultimately leading to the loss of photoreceptor function.[1] More than 30 million patients worldwide are currently suffering from retinal degenerative diseases.[2] Currently, there are many treatment strategies designed to delay the disease progression, such as gene therapies, administration of growth factors, and antiangiogenic therapies. One of the most promising therapies for late-stage retinal degeneration is to deliver retinal stem or progenitor cells to the subretina.[3,4] Several studies indicate that a typical bolus injection of mouse retinal progenitor cells (mRPCs) leads to massive new cell loss through efflux and death.[3,5] Recently it was demonstrated that a tissue engineering approach, the usage of a biocompatible polymer scaffold, improved the mRPCs survival and promoted the integration of transplanted mRPCs in host retinal tissue following transplantation.[5–8]

Electrospinning is a unique and versatile technique capable of producing fibers as small as 5 nm and has been used to produce nanofibrous scaffolds which mimic natural extracellular matrix important for organizing cells and providing signals for cellular responses.[9–14]

Chitosan (CS), a fully or partially deacetylated chitin, has been used in a number of biomedical applications, such as drug-delivery systems, wound dressings, and nerve regeneration agents, due to its high biocompatibility, low toxicity, and

Corresponding: Ping Gu
Department of Ophthalmology, Shanghai Ninth People's Hospital, School of Medicine, Shanghai Jiaotong University, Shanghai 200011, China
Tel +86 21 6313 5606
Fax +86 21 6313 7148
Email guping06@gmail.com

antimicrobial properties.[15–20] Despite the promising potential of chitosan, its poor electrospinnability, insolubility in common organic solvents, and high brittleness have hampered its basic research and applications.[16,17,21] Poly(ε-caprolactone) (PCL), a semicrystalline biodegradable polyester, has received US Food and Drug Administration approval for several clinical applications for humans, and it is also a commonly used scaffold for tissue engineering due to its high biocompatibility, mechanical properties, and nontoxicity.[22–24] However, the drawbacks of PCL, such as its strong hydrophobicity, slow degradation kinetics, and lack of bioactive functions, have greatly limited its application as scaffolds in tissue engineering.[16,17] Therefore, blending the bioactive functions of chitosan with the good mechanical properties of PCL to generate a new biohybrid material should show an improvement in biological, mechanical, and degradation properties compared with the individual components. Solvent systems like trifluoroacetic acid[19] and hexafluoro-2-propanol[25] have been employed to fabricate CS/PCL nanofibrous scaffolds. However, all these solvents are relatively expensive compared with conventional solvent systems, and their nature may result in faster degradation of the polymers.[26]

In this work, a CS-PCL copolymer was first prepared by grafting ε-caprolactone oligomers onto the hydroxyl groups of CS via ring-opening polymerization which was then blended with PCL to yield a 3-dimensional CS-PCL/PCL scaffold. The hypothesis was that the CS-PCL/PCL scaffolds would be easily fabricated by electrospinning their blend solutions in a common solvent system. Furthermore, it was expected that the grafting modification of CS improved the interfacial adhesion with the PCL fiber matrix.[27] Its properties, such as wettability, surface topography, and porosity of the CS-PCL/PCL scaffolds were characterized. To study the cellular compatibility of the nanofibrous structure for potential applications in retinal tissue engineering, mRPCs were cultured on the scaffolds, and their cell proliferation and differentiation were evaluated.

Materials and methods

Materials

All reagents and chemicals were of analytical grade and used without further purification unless otherwise stated. CS (degree of deacetylation (DD) >85%) was purchased from Golden-shell Biochemical Company (Zhejiang, China). PCL (Mw, 80 kDa) was obtained from Chunshin Chemical Company (Shanghai, China). Methanesulfonic acid ($MeSO_3H$, >99.5%) and ε-caprolactone (ε-CL) were purchased from Sigma-Aldrich (St Loius, MO).

Preparation of CS-PCL copolymer

CS-PCL was synthesized by grafting ε-caprolactone oligomers onto CS via ring-opening polymerization.[28,29] Briefly, CS (2.0 g, 12 mmol of glucosamine units, taking into account DD) and 20 mL of $MeSO_3H$ was charged into a flame-dried 50 mL round-bottom flask equipped with a Teflon-coated stir bar and gas adaptor, and rubber septum. The mixture was stirred at 45°C for about 30 minutes to allow CS to completely dissolve, followed by the injection of ε-CL monomer (16.58 g, 145 mmol). The reaction mixture was stirred for 5 hours under nitrogen atmosphere at 45°C. After filtration, the filtrate was dropped into a solution containing 250 mL of 0.2 M KH_2PO_4, 40 mL of 10 M NaOH, and 100 g of crushed ice. The resulting copolymer was collected by filtration, washed with distilled water several times, dialyzed with a membrane (Spectra/Pro, MWCO = 3500) against deionized water at 4°C for 48 hours, and freeze-dried under vacuum at −56°C for 3 days.

After preparing the copolymer, its properties such as molecular weight and average number of ε-CL units grafted onto one glucosamine unit in CS (CL_n) were detected and summarized in Table 1. CL_n was determined by proton nuclear magnetic resonance (^{1}H NMR) using the following equation:

$$CL_n = A_{[(a)/2]}/A_{[(3, 4, 5, 6, 6')/5]},$$

where $A_{[(a)/2]}$ and $A_{[(3, 4, 5, 6, 6')/5]}$ represent half of the integral area of protons in PCL units at 2.2 ppm and one-fifth of the total integral area of proton 3, 4, 5, 6, and 6′ of saccharine units in CS at 3.4–3.9 ppm, respectively.

NMR

^{1}H NMR spectra of the CS-PCL copolymer was obtained by dissolving the sample in deuterated dimethyl sulfoxide (DMSO-d_6) and analyzed on an Avance™ 500 NMR spectrometer (Bruker, Billerica, MA). Tetramethylsilane was used as an internal standard.

Table 1 Characterization of CS-PCL

Sample	MFR[a]	Yield (%)[b]	Mw (×10⁴)[c]	PDI[c]	CL_n[d]
CS-PCL	12	79	4.86	3.43	2.7

Notes: [a]Moral feed ratio of ε-CL to glucosamine units; [b]Yield (%) = $[(W_{CS\text{-}PCL})/(W_{CL} + W_{CS})] \times 100\%$; [c]Measured by GPC; polystyrene samples were used as standard; [d]Average number of ε-CL units per glucosamine unit in CS, $CL_n = A_{[(a)/2]}/A_{[(3, 4, 5, 6, 6')/5]}$, calculated from ^{1}H NMR.

Abbreviations: ^{1}H NMR, proton nuclear magnetic resonance; CL, caprolactone; CS, chitosan; CS-PCL, cationic chitosan-graft-poly (ε-caprolactone); GPC, gel permeation chromatography; MFR, moral feed ratio; Mw, molecular weight; PDI, polydispersity index.

Fourier-transform infrared

Samples were mixed with KBr, pressed into a slice and then recorded on a Fourier-transform infrared (FT-IR) spectrometer (Nicolet 6700; Nicolet, Madison, WI) in the range of 4000–400 cm^{-1}.

Preparation of nanofibrous scaffolds from PCL and CS-PCL/PCL by electrospinning

PCL (15 wt %) was dissolved in chloroform/methanol (4:1 v/v) and used for electrospinning to obtain PCL nanofibers. To prepare CS-PCL/PCL nanofibers, PCL and CS-PCL solutions were prepared separately by dissolving PCL or CS-PCL in dimethylformamide/chloroform (1:4 v/v). PCL and CS-PCL solutions of different proportions were then mixed to obtain mixtures with different weight ratios of CS-PCL to PCL. The resultant mixtures were stirred for 24 hours to obtain homogenous solutions. For electrospinning, PCL or CS-PCL/PCL solutions were placed into a 5 mL standard syringe equipped with a 27G blunted stainless steel needle using a syringe pump (LSP02-1B; Baoding Longer Precision Pump Co, Ltd, Baoding, China) at a rate of 1.0 mL/h with an applied voltage of 13 KV (DW-P303-1ACD8; High Voltage Research, Tianjin, China). A flat aluminum plate was kept 12 cm from the syringe needle tip for collecting the fibers. The electrospun samples were vacuum dried for 3 days to remove any solvent residues.

Characterization of electrospun nanofibrous scaffolds

The morphology of electrospun nanofibrous scaffolds was observed under a scanning electron microscopy (SEM) after sputter coating with platinum (Pt). The average diameter of electrospun nanofibers was determined by measuring at least 20 different fibers and 100 different segments in SEM images, and five images were used for each fiber sample.[30] The thickness of the nanofibrous scaffolds was measured by a micrometer, and its apparent density and porosity were calculated using the following equations.[31]

$$\text{Apparent density } (g/cm^3) = \frac{\text{mass of scaffold (g)}}{\text{scaffold thickness (cm)} \times \text{scaffold area } (cm^2)}$$

$$\text{Scaffold porosity} = \left(1 - \frac{\text{apparent density } (g/cm^3)}{\text{buck density of CS-PCL/PCL } (g/cm^3)}\right) \times 100\%$$

The wettability of electrospun scaffolds was assessed by the sessile drops water contact angle measurement using a contact angle and surface free energies analyzer (OCA15; DataPhysics, Filderstadt, Germany). Distilled water was used as the testing liquid. Each experiment was carried out at room temperature and repeated 10 times. Means were shown as results.

The surface chemistry of electrospun scaffolds was determined by X-ray photoelectron spectroscopy (XPS) using an RBD upgraded PHI-5000C ESCA system (Perkin Elmer, Waltham, MA) with Mg Kα radiation (hν = 1253.6 eV). Binding energy was referenced to the C1s peak of saturated hydrocarbon at 285.0 eV.

The zeta-potential (ζ) measurements of electrospun fibers in aqueous phase were conducted by dynamic light scattering (DLS) (Zetasizer Nano ZS; Malvern Instruments, Malvern, UK) at room temperature. Data are presented as means and corresponding standard deviations (mean ± SD) from five independent experiments.

Isolation and culture of mRPCs

RPCs were previously isolated from the neural retina of postnatal day one green fluorescent protein (GFP) transgenic mice.[32] The GFP transgenic C57BL/6 mice were produced with an enhanced GFP cDNA under the control of a chicken beta-actin promoter and cytomegalovirus enhancer. Retinas were harvested from newborn GFP transgenic C57BL/6 mice (gift from Masaru Okabe, University of Osaka, Osaka, Japan) and subjected to 0.1% type I collagenase (Invitrogen, Carlsbad, CA) digestion to dissociate the tissue. Single cell suspension was achieved by passing the digested tissue through a nylon mesh. The final cell suspension was cultured in medium, consisting of advanced Dulbecco's modified Eagle's medium: nutrient mixture F-12 (DMEM/F12) (Invitrogen), 1% N2 neural supplement (Invitrogen), 2 mM L-glutamine (Invitrogen), 100 U/mL penicillin–streptomycin (Invitrogen), and 20 ng/mL epidermal growth factor (recombinant human EGF) (Invitrogen). Cultured medium was changed every 2 days. GFP^+ clusters (neurospheres) appeared within the first 2–3 days, and cells were passaged at regular intervals of 4–5 days. These cells were immunoreactive for nestin (a marker for neural progenitor cells) and proliferation marker Ki-67.

Cell seeding and culture

Each of the nanofibrous scaffolds was sterilized under an ultraviolet lamp for 30 minutes (15 min/side) at room temperature before being placed into 24-well culture

plates. Specimens were rinsed three times with sterilized phosphate-buffered solution (PBS), and incubated with 40 μg/mL mouse laminin (Sigma-Aldrich) in PBS for 2 hours at 37°C. Scaffolds were then rinsed three times with PBS and immersed in culture medium for 2 hours at 37°C prior to cell seeding. Cultured GFP+ mRPCs were dissociated into single cell suspensions and seeded at a density of 3×10^4/well onto polymer scaffolds with a total volume of 1 mL of culture medium. mRPCs were allowed to proliferate on polymer scaffolds for 7 days.

Cell proliferation

To visualize the expansion of GFP+ mRPCs on the electrospun scaffolds, cultures were imaged at 10× magnification using a standard epifluorescence microscope (Olympus IX51; Olympus, Tokyo, Japan) on days 1, 4, and 7. The proliferation of mRPCs on different substrates was further investigated by MTS (3-(4,5-dimethylthiazol-2-yl)-5-(3-carboxymethoxyphenyl)-2-(4-sulfophenyl)-2H-tetrazolium) assay (CellTiter 96 Aqueous One Solution; Promega, Madison, WI). The cellular constructs were rinsed with PBS followed by incubation with 20% of MTS reagent for 4 hours at 37°C according to the reagent instructions. The incubated suspension was then pipetted into a 96-well plate, and the absorbance was read at 490 nm using a microplate reader (ELX800; BioTeK, Winooski, VT).

Morphology of mRPCs on electrospun scaffolds

Morphology of mRPCs on the scaffolds was imaged using an SEM. At the predetermined time points of 1, 4, and 7 days, the cell-cultured scaffolds were fixed in 4% glutaraldehyde for 2 hours at 4°C. Following three rinses with distilled water, the samples were dehydrated through a series of graded ethanol and then freeze-dried. Dry constructs were sputter coated with Pt and observed on an SEM (JSM-6701; JEOL, Tokyo, JAPAN).

RNA isolation

Total RNA was extracted from each sample using the RNeasy Mini Kit (Qiagen, Valencia, CA). RNA samples were treated by DNaseI (Qiagen) to digest and eliminate any contaminating genomic DNA. RNA concentration was measured at a wavelength of 260 nm (A260) and the purity of total RNA was determined by the A260/A280 ratio. Quantitative polymerase chain reaction (qPCR) analyses were only performed on samples with A260/A280 ratios between 1.9 and 2.1.

Reverse transcription and qPCR

Two micrograms of total RNA in a 20 μL reaction volume were reverse transcribed using the PrimeScript™ RT reagent Kit (Perfect Real Time; TaKaRa, Dalian, China). A primer set for each gene was designed using Primer3 software (see http://frodo.wi.mit.edu/cgi-bin/). qPCR was performed using a 7500 Real-Time PCR Detection System (Applied Biosystems, Carlsbad, CA) in 20 μL total volume containing 10 μL of 2× SYBR PCR Premix EX Taq™ (Perfect Real Time; TaKaRa), 10 μL of cDNA, and 300 nM of gene-specific primers (Table 2). The cycling parameters for qPCR were as follows: initial denaturation at 95°C for 10 minutes, followed by 40 cycles of 15 seconds at 95°C and 1 minute at 60°C. β-actin (endogenous control) was selected for normalization of gene expression. The PCR efficiency of the reaction was measured with primers by using serial dilution of cDNA (1:1, 1:5, 1:25, 1:125, 1:625, and 1:3,125). The relative expression of the gene of interest, (Etarget) ΔCt target (control-treated)/(Eref)ΔCt ref (control-treated), was then evaluated by

Table 2 Primers used for quantitative qPCR

Genes	Accession number	Forward (5′–3′)	Reverse (5′–3′)	Annealing temperature (°C)	Product size (base pairs)
Nestin	NM_016701	aactggcacctcaagatgt	tcaagggtattaggcaagggg	60	235
Vimentin	NM_011701	tggttgacacccactcaaaa	gcttttggggtgtcagttgt	60	269
Ki-67	X82786	cagtactcggaatgcagcaa	cagtcttcaggggctctgtc	60	170
β3-tubulin	NM_023279	cgagacctactgcatcgaca	cattgagctgaccagggaat	60	152
Map2	NM_001039934	agaaaatggaagaaggaatgactg	acatggatcatctggtacctttt	60	112
Recoverin	NM_009038	atggggaatagcaagagcgg	gagtccgggaaaaacttggaata	60	179
Rhodopsin	NM_145383	tcaccaccaccctctacaca	tgatccaggtgaagaccaca	60	216
PKC-α	NM_011101	cccattccagaaggagatga	ttcctgtcagcaagcatcac	60	212
GFAP	NM_010277	agaaaaccgcatcaccattc	tcacatcaccacgtccttgt	60	184
β-actin	NM_007393	agccatgtacgtagccatcc	ctctcagctgtggtggtgaa	60	152
Caspase 3	NM_009810	aaggagcagctttgtgtgtgt	cgcctctgaagaagctagtca	60	107

Abbreviations: GFAP, glial fibrillary acidic protein; PKC-α, protein kinase C alpha; qPCR, polymerase chain reaction.

the Pfaffl method.[33] The cycle threshold (Ct) value represents the number of PCR cycles at which an increase in fluorescence signal (and therefore cDNA) is able to be detected above the background and the increase is exponential for the particular gene. Data are expressed as fold change relative to untreated controls, after normalizing to β-actin.

Statistical analysis

All data presented in this study are shown as mean ± standard deviation (SD) unless specifically indicated otherwise. Each experiment was repeated for at least three times. Statistical analyses were performed on the data obtained using a one-way ANOVA, and when a value of $P \leq 0.05$, the difference was considered statistically significant.

Results and discussion

Synthesis of CS-PCL copolymer

The structures of CS, PCL, and CS-PCL were detected by ^{1}H NMR as shown in Figure 1. As demonstrated in Figure 1A, ^{1}H NMR chemical shifts at 3.4–3.9, 3.2, and 2.05 ppm were assigned to $H_{3, 4, 5, 6, 6'}$, $H_{2'}$ and H_7 of pyranose repeat units in CS, respectively. The characteristic peaks of the PCL chain appear at 2.2 ppm (H_a), 1.6–1.7 ppm ($H_{b, d}$), 1.4 ppm (H_c), and 4.15 ppm (H_e). Hence, the PCL was covalently grafted to CS to form the CS-PCL copolymers which were identified by the presence of the characteristic peaks of CS and PCL in its ^{1}H NMR spectrum.[34] The structure of CS-PCL was further analyzed by FT-IR spectra. As shown in Figure 2C, CS showed the characteristic bands of saccharine structure at 890 and 1147 cm^{-1}. The absorbance of amide I band and amino groups in CS was shown at 1664 and 1616 cm^{-1},[28] respectively. The ester stretching of PCL at 1734 cm^{-1} was observed as a characteristic peak on PCL (Figure 2B).

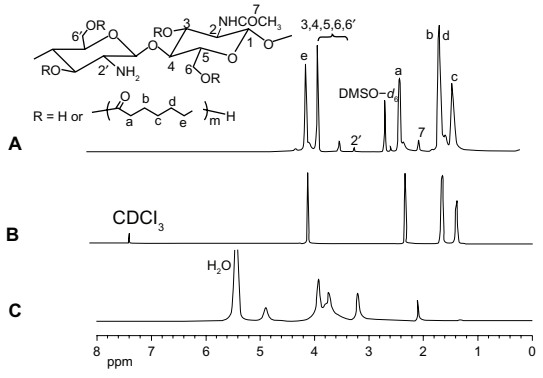

Figure 1 Proton nuclear magnetic resonance spectra of CS-PCL (**A**), PCL (**B**), and CS (**C**).
Abbreviations: CS, chitosan; CS-PCL, cationic chitosan-graft-poly (ε-caprolactone); DMSO, dimethyl sulfoxide; PCL, polycaprolactone.

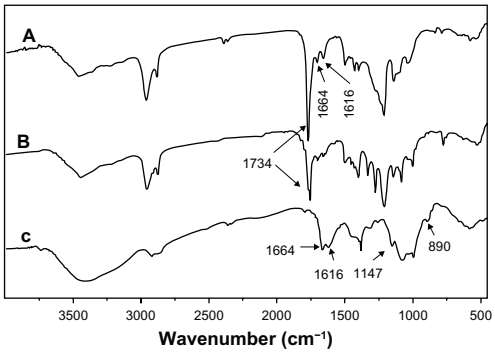

Figure 2 Fourier-transform infrared spectra of CS-PCL (**A**), PCL (**B**), and CS (**C**).
Abbreviations: CS, chitosan; CS-PCL, cationic chitosan-graft-poly (ε-caprolactone); PCL, polycaprolactone.

The FT-IR spectra of CS-PCL (Figure 2A) exhibited absorbance bands at 1734, 1664, and 1616 cm^{-1}, which were assigned to the characteristic bands of ester in PCL, amide I band, and amino groups in CS, respectively. This implied the successful graft copolymerization of CL onto CS, along with the unreactioned amino groups of CS.

Fiber preparation and characterization

Previous studies have shown that the morphology of electrospun nanofibers is highly influenced by various parameters such as applied voltage, distance between the needle tip and collector, and especially properties of polymer solutions including surface tension, viscosity, and the nature of solvent.[35,36] Figure 3 shows SEM micrographs of the nanofibers obtained at different weight ratios of CS-PCL/PCL. At a CS-PCL/PCL ratio of 100:0, fibers did not form (Figure 3A). When a small portion of PCL was added into the solution of CS-PCL, as shown in Figure 3B (CS-PCL/PCL (80/20), beads were deposited on the collector and fibers began to form. As the proportion of PCL solution increased (CS-PCL/PCL (60/40)), the size of the

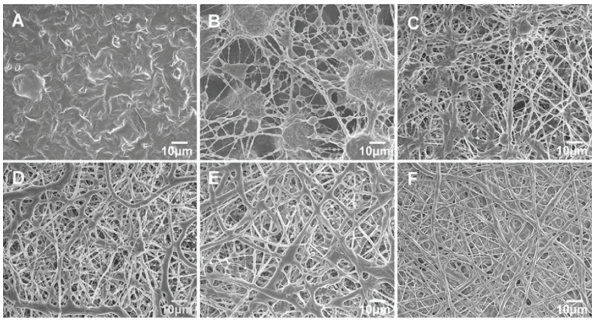

Figure 3 Scanning electron microscopy images of electrospun nanofibous scaffolds prepared from different CS-PCL/PCL weight ratios: CS-PCL (**A**), CS-PCL/PCL (80/20) (**B**), CS-PCL/PCL (60/40) (**C**), CS-PCL/PCL (40/60) (**D**), CS-PCL/PCL (20/80) (**E**), and PCL (**F**).
Abbreviations: CS-PCL, cationic chitosan-graft-poly (ε-caprolactone); PCL, polycaprolactone.

beads became smaller and fibers coexisted among the beads (Figure 3C). When the CS-PCL/PCL ratio reached up to 40/60, homogeneous fibers could be spun (Figure 3D). As the amount of the PCL solution was further increased in the blended solution, the electrospinning process became more and more fluent (Figures 3E and 3F). The average fiber diameters, as estimated from the images, were summarized in Table 3. When the content of PCL in the blends increased from 60% to 100%, the mean diameter of blended nanofibers gradually increased from 656 ± 53 to 925 ± 42 nm. The porosities of blended nanofibers also increased from 77% to 89% (Table 3). Highly porous structures obtained from these electrospun scaffolds were desirable since high porosities impart large surface area and make more room for cell adhesion and migration.[37]

The cell adhesion, proliferation, and differentiation on a polymer surface are affected by the wettability of a polymer surface.[38,39] Water contact angles (WCA) for the CS-PCL/PCL and PCL electrospun scaffolds are summarized in Table 3. The water contact angle for PCL electrospun scaffold was about 134° ± 2°, which indicates that the PCL electrospun scaffold has hydrophobic properties. In contrast, all the CS-PCL/PCL electrospun scaffolds were highly hydrophilic with a contact angle of 0° due to the presence of hydrophilic amino groups and hydroxyl groups on their surface.

Studies on the surface chemistry of the electropun scaffolds were performed by XPS. Table 4 shows the atomic ratios (%) of C1s, N1s, and O1s on the surfaces of CS-PCL/PCL and PCL nanofibrous scaffolds. The percentage of N on the fiber surface climbed as the amount of CS-PCL increased in the spinning solution. Nitrogen atoms were not present within the chemical composition of PCL scaffolds, whereas they were present in CS-PCL/PCL scaffolds. The latter was due to the presence of CS-PCL molecules on the surface of CS-PCL/PCL nanofibrous scaffolds. The presence of N1s peak at 395.1 eV in the XPS spectra of CS-PCL/PCL (XPS spectrum not shown here) nanofibrous scaffolds confirmed it. No nitrogen peak was observed in the surface scan of XPS spectra of PCL scaffolds. The XPS results indicated that amino groups were present on the surface of CS-PCL/PCL nanofibrous scaffolds. This was consistent with its high hydrophilicity shown by the water contact angle for CS-PCL/PCL scaffolds.

Table 3 Fiber diameter, porosity, and water contact angle properties of different electrospun nanofibrous scaffolds

Sample	Fiber diameter	Porosity	WCA
CS-PCL/PCL (40/60)	656 ± 53 nm	77% ± 6%	0°
CS-PCL/PCL (20/80)	775 ± 35 nm	84% ± 4%	0°
PCL	925 ± 42 nm	89% ± 3%	134° ± 2°

Abbreviations: CS-PCL, cationic chitosan-graft-poly (ε-caprolactone); PCL, polycaprolactone; WCA, water contact angle.

Table 4 Atomic ratios of carbon, nitrogen, and oxygen on the surface of CS-PCL/PCL (40/60), CS-PCL/PCL (20/80), and PCL nanofibrous scaffolds determined by x-ray photoelectron spectroscopy

Nanofibers	Carbon ratio (%)	Nitrogen ratio (%)	Oxygen ratio (%)
CS-PCL/PCL (40/60)	74.38	0.31	25.31
CS-PCL/PCL (20/80)	74.64	0.24	25.12
PCL	75.54	0	24.46

Abbreviations: CS-PCL, cationic chitosan-graft-poly (ε-caprolactone); PCL, polycaprolactone.

The zeta-potential of electrospun fibers in an aqueous phase cling to the type and the density of ionizable or polar functional groups of polymers.[40] To understand the effect of the CS-PCL/PCL nanofibers composition on zeta-potential, the zeta-potential of CS-PCL/PCL nanofibers with various CS-PCL ratios was detected by DLS. Figure 4 shows that the zeta-potential of PCL nanofibers is negative (–12 mV), whereas CS-PCL/PCL nanofibers display a positive zeta-potential. PCL fibers have a negative surface charge due to the orientation of their carbonyl groups on the surface of nanofibers.[40] In the case of CS-PCL/PCL scaffolds, the positive zeta-potential of CS-PCL/PCL scaffolds is attributed to the dominance of amino groups in CS-PCL present on the surface. With dramatically increasing CS-PCL percentages from 10% to 80%, zeta-potential obtained for CS-PCL/PCL nanofibers ranged from –3 to +50 mV. Positive zeta-potential of materials used as tissue engineering scaffolds is necessary for the attachment to anionic cell surfaces, which consequently facilitates cell adhesion on its surface.[41]

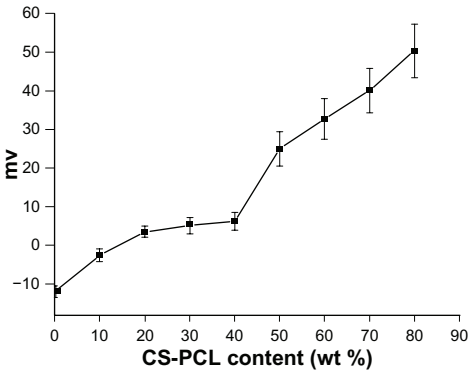

Figure 4 Zeta-potential curve for electrospun nanofibrous scaffolds (n = 5).
Abbreviation: CS-PCL, cationic chitosan-graft-poly (ε-caprolactone).

Cell proliferation on electrospun scaffolds

Figure 5 shows a fluorescent micrograph of GFP+ mRPCs on different substrates at days 1, 4, and 7 after cell seeding. Generally, it revealed that cell numbers increased steadily on all scaffolds studied during the culture time. However, the cell density of mRPCs on CS-PCL/PCL (20/80) was obviously higher compared with that on CS-PCL/PCL (40/60) or PCL scaffolds after 7 days in culture. This result was further confirmed by MTS assay (Figure 6). As shown in Figure 6, mRPCs cultured on both CS-PCL/PCL (20/80) and CS-PCL/PCL (40/60) scaffolds proliferated faster than on PCL scaffolds. This could be attributed to amino groups on the CS-PCL, which impart more hydrophilic sites on CS-PCL/PCL scaffolds. This results in more suitable conditions for cell growth and proliferation. Gupta et al demonstrated that Schwann cells preferred to attach to PCL/gelatin scaffolds with a hydrophilic surface than PCL scaffolds with a hydrophobic surface.[37] However, our studies showed that the numbers of mRPCs on CS-PCL/PCL (20/80) scaffolds increased not only faster than that on PCL scaffolds but also faster than on CS-PCL/PCL (40/60) scaffolds. The latter may attribute to the relative higher zeta-potential of CS-PCL (40/60) scaffolds, which may play a negative impact on the cell surface leading to lower proliferation. A similar result was reported by Zhu and his co-workers, who investigated the cytocompatibility of human endothelial cells on an aminolyzed polycaprolactone membrane. They demonstrated that the introduction of amino groups on the surface of PCL membrane has a positive effect on improving cytocompatibility only to a limited extent.[41] In conclusion, our results indicated that CS-PCL/PCL (20/80) scaffolds best supported mRPCs growth compared with the other electrospun scaffolds.

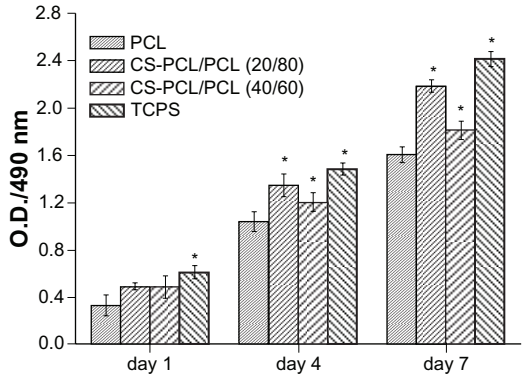

Figure 6 Analysis of mRPC proliferation on PCL and CS-PCL/PCL nanofibrous scaffolds and the cell culture plates (TCPS), measured by MTS assay.
Notes: Bar represents mean ± standard deviation (n = 4). *$P < 0.05$.
Abbreviations: CS-PCL, cationic chitosan-graft-poly (ε-caprolactone); mRPC, mouse retinal progenitor cell; MTS, 3-(4,5-dimethylthiazol-2-yl)-5-(3-carboxymethoxyphenyl)-2-(4-sulfophenyl)-2H-tetrazolium; OD, optical density; PCL, polycaprolactone; TCPS, tissue culture polystyrene.

Cell morphology

To visualize the morphology of the mRPCs seeded into electrospun scaffolds, SEM images were taken after

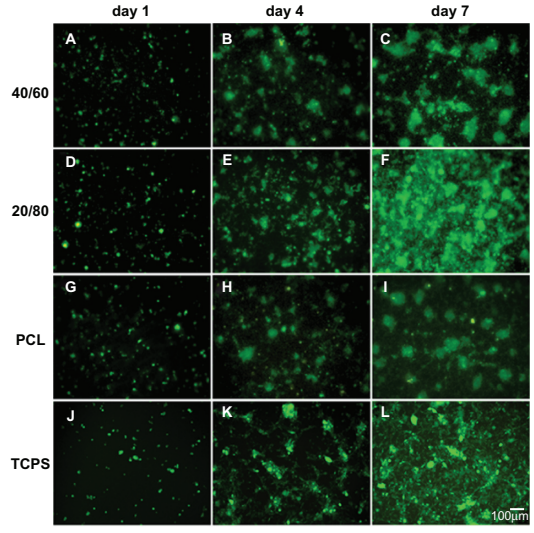

Figure 5 Fluorescent micrograph of mRPC density on CS-PCL/PCL (40/60) (**A–C**), CS-PCL/PCL (20/80) (**D–F**), PCL (**G–I**) nanofibrous scaffolds, and the cell culture plates (TCPS) (**J–L**) on day 1, 4, and 7 after incubation (green = endogenous GFP expression). Scale bar: 100 μm.
Abbreviations: CS-PCL, cationic chitosan-graft-poly (ε-caprolactone); GFP, green fluorescent protein; PCL, polycaprolactone; mRPC, mouse retinal progenitor cell; TCPS, tissue culture polystyrene.

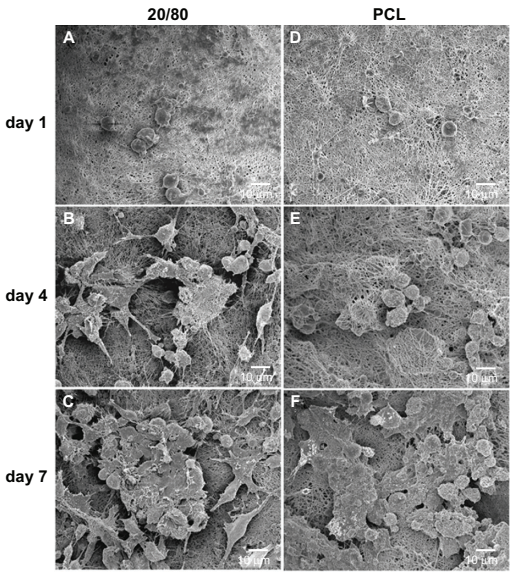

Figure 7 Scanning electron microscopy images of mRPCs grown on CS-PCL/PCL (20/80) (**A–C**) and PCL (**D–F**) nanofibrous scaffolds on day 1 (**A, D**), 4 (**B, E**), and 7 (**C, F**) after incubation.
Abbreviations: CS-PCL, cationic chitosan-graft-poly (ε-caprolactone); mRPC, mouse retinal progenitor cell; PCL, polycaprolactone.

1, 4, and 7 days of culture (Figure 7). With time, in culture, mRPCs grown on PCL scaffolds adopted a spherical morphology. In contrast, there were more cells observed on CS-PCL/PCL (20/80) scaffolds that possessed neuron-like morphology with bipolar or multipolar extensions. Compared with PCL scaffolds, the CS-PCL/PCL (20/80) scaffolds provided a better niche for mRPC differentiation towards a neuron-like phenotype. It could be inferred that the presence of amino groups on the surfaces of CS-PCL/PCL (20/80) scaffolds partly support the neuronal differentiation of mRPCs. Yang et al,[25] who cultured mouse preosteoblast cells on chitosan containing nanofibrous scaffolds, demonstrated a similar result: that the scaffolds could accelerate the osteogenic differentiation of preosteoblasts.

Gene expression

The expression of 10 key genes involved in retinal development was examined by qPCR in mRPCs grown on electrospun scaffolds. The expression level for each gene in mRPCs grown without nanofibrous scaffold treatment was defined as 1. As shown in Figure 8, five retinal neuronal markers (β3-tubulin, map2, recoverin, rhodopsin, protein kinase C [PKC]-α) showed notably higher expression in mRPCs grown on the CS-PCL/PCL (20/80) scaffolds compared with PCL scaffolds. In contrast, the expression level for glial fibrillary acidic protein (GFAP), which is involved in the development of glial cells, was much lower in mRPCs grown on CS-PCL/PCL (20/80) scaffold cells as compared with PCL scaffold cells. These results indicate that mRPCs grown on CS-PCL/PCL (20/80) scaffolds are more likely to differentiate towards neuronal lineage while mRPCs grown on PCL scaffolds preferentially differentiate into glia. In addition, when compared with controls, mRPCs grown on CS-PCL/PCL (20/80) scaffold did not exhibit notable differences in expression levels of nestin (retinal progenitor marker), vimentin (retinal progenitor marker), Ki-67 (cell proliferation marker), and caspase 3 (cell apoptotic marker) suggesting that mRPCs grew well on the scaffolds. Collectively, this data suggests the CS-PCL/PCL (20/80) nanofibers could be used as a potential scaffold for mRPC growth and neuronal differentiation.

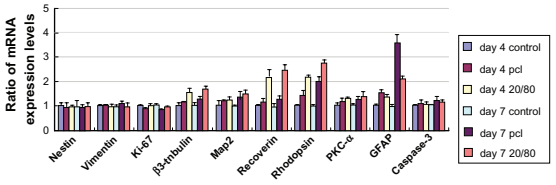

Figure 8 Gene expression profile of mRPCs grown on CS-PCL/PCL (20/80) and PCL scaffolds on day 4 and 7.
Note: The error bars show standard deviation (n = 3).
Abbreviations: CS-PCL, cationic chitosan-graft-poly (ε-caprolactone); GFAP, glial fibrillary acidic protein; mRPC, mouse retinal progenitor cell; PCL, polycaprolactone; PKC-α, protein kinase C alpha.

Conclusion

Nanofibrous scaffolds of CS-PCL/PCL were easily fabricated by electrospinning. The diameters of the CS-PCL/PCL electrospun nanofibrous ranged from 656 ± 53 to 925 ± 42 without bead formation. Results of XPS analysis and zeta-potential measurements of CS-PCL/PCL scaffolds suggested the presence of amino groups on their surface, which results in high hydrophilicity. In particular, the CS-PCL/PCL (20/80) nanofibrous scaffold favored mRPC proliferation and differentiation toward neuronal lineage and could be a potential bioengineering material for retinal tissue repair.

Acknowledgments

The authors are grateful to Dr Henry Klassen and Dr Michael J Young for original provenance of the murine RPCs. The research work was supported by Shanghai Municipality Commission for Science and Technology (09PJ1407200, 0952nm05300), International Corporation Project of Shanghai Municipality Commission (09540709000, 10410710000), Education Commission of Shanghai (11YZ47), National Natural Science Foundation of China (81070737), Shanghai Leading Academic Discipline Project (S30205).

Disclosure

The authors report no conflicts of interest in this work.

References

1. Margalit E, Sadda SR. Retinal and optic nerve diseases. *Artif Organs*. 2003;27(11):963–974.
2. Ambati J, Ambati BK, Yoo SH, Ianchulev S, Adamis AP. Age-related macular degeneration: etiology, pathogenesis, and therapeutic strategies. *Surv Ophthalmol*. 2003;48(3):257–293.
3. Klassen HJ, Ng TF, Kurimoto Y, et al. Multipotent retinal progenitors express developmental markers, differentiate into retinal neurons, and preserve light-mediated behavior. *Invest Ophthalmol Vis Sci*. 2004;45(11):4167–4173.
4. Redenti S, Neeley WL, Rompani S, et al. Engineering retinal progenitor cell and scrollable poly (glycerol-sebacate) composites for expansion and subretinal transplantation. *Biomaterials*. 2009;30(20):3405–3414.
5. Lavik EB, Klassen H, Warfvinge K, Langer R, Young MJ. Fabrication of degradable polymer scaffolds to direct the integration and differentiation of retinal progenitors. *Biomaterials*. 2005;26(16):3187–3196.
6. Tao SL, Desai TA. Aligned arrays of biodegradable poly (ε-caprolactone) nanowires and nanofibers by template synthesis. *Nano Lett*. 2007;7(6):1463–1468.
7. Neeley WL, Redenti S, Klassen H, et al. A microfabricated scaffold for retinal progenitor cell grafting. *Biomaterials*. 2008;29(4):418–426.
8. Redenti S, Tao S, Yang J, et al. Retinal tissue engineering using mouse retinal progenitor cells and a novel biodegradable, thin-film poly (ε-caprolactone) nanowire scaffold. *J Ocul Biol Dis Infor*. 2008;1(1):19–29.

9. Vasita R, Katti DS. Nanofibers and their applications in tissue engineering. *Int J Nanomedicine*. 2006;1(1):15–30.
10. Zhang YZ, Su B, Venugopal J, Ramakrishna S, Lim CT. Biomimetic and bioactive nanofibrous scaffolds from electrospun composite nanofibers. *Int J Nanomedicine*. 2007;2(4):623–638.
11. Gelain F. Novel opportunities and challenges offered by nanobiomaterials in tissue engineering. *Int J Nanomedicine*. 2008;3(4):415–424.
12. Prabhakaran MP, Venugopal J, Chan CK, Ramakrishna S. Surface modified electrospun nanofibrous scaffolds for nerve tissue engineering. *Nanotechnology*. 2008;19(45):455102.
13. Gupta D, Venugopal J, Mitra S, Giri Dev VR, Ramakrishna S. Nanostructured biocomposite substrates by electrospinning and electrospraying for the mineralization of osteoblasts. *Biomaterials*. 2009;30(11):2085–2094.
14. Valmikinathan CM, Defroda S, Yu X. Polycaprolactone and bovine serum albumin based nanofibers for controlled release of nerve growth factor. *Biomacromolecules*. 2009;10(5):1084–1089.
15. Wang YC, Kao SH, Hsieh HJ. A chemical surface modification of chitosan by glycoconjugates to enhance the cell-biomaterial Interaction. *Biomacromolecules*. 2003;4(2):224–231.
16. Sarasam A, Madihally SV. Characterization of chitosan-polycaprolactone blends for tissue engineering applications. *Biomaterials*. 2005;26(27):5500–5508.
17. Feng H, Dong CM. Preparation and characterization of chitosan-graft-poly (ε-caprolactone) with an organic catalyst. *J Polym Sci A Polym Chem*. 2006;44(18):5353–5361.
18. Zhang YZ, Su B, Ramakrishna S, Lim CT. Chitosan nanofibers from an easily electrospinnable UHMWPEO-doped chitosan solution system. *Biomacromolecules*. 2007;9(1):136–141.
19. Prabhakaran MP, Venugopal JR, Chyan TT, et al. Electrospun biocomposite nanofibrous scaffolds for neural tissue engineering. *Tissue Eng Part A*. 2008;14(11):1787–1797.
20. Haider S, Park SY. Preparation of the electrospun chitosan nanofibers and their applications to the adsorption of Cu (II) and Pb (II) ions from an aqueous solution. *J Memb Sci*. 2009;328(1–2):90–96.
21. Klossner RR, Queen HA, Coughlin AJ, Krause WE. Correlation of chitosan's rheological properties and its ability to electrospin. *Biomacromolecules*. 2008;9(10):2947–2953.
22. Paneva D, Bougard F, Manolova N, Dubois P, Rashkov I. Novel electrospun poly (ε-caprolactone)-based bicomponent nanofibers possessing surface enriched in tertiary amino groups. *Eur Polym J*. 2008;44(3):566–578.
23. Chang KY, Cheng LW, Ho GH, Huang YP, Lee YD. Fabrication and characterization of poly (gamma-glutamic acid)-graft-chondroitin sulfate/polycaprolactone porous scaffolds for cartilage tissue engineering. *Acta Biomater*. 2009;5(6):1937.
24. Kim JH, Choung PH, Kim IY, et al. Electrospun nanofibers composed of poly (ε-caprolactone) and polyethylenimine for tissue engineering applications. *Mater Sci Eng C*. 2009;29(5):1725–1731.
25. Yang X, Chen X, Wang H. Acceleration of osteogenic differentiation of preosteoblastic cells by chitosan containing nanofibrous scaffolds. *Biomacromolecules*. 2009;10(10):2772–2778.
26. Shalumon KT, Anulekha KH, Girish CM, Prasanth R, Nair SV, Jayakumar R. Single step electrospinning of chitosan/poly(caprolactone) nanofibers using formic acid/acetone solvent mixture. *Carbohydr Polym*. 2010;80(2):413–419.
27. Zoppe JO, Peresin MS, Habibi Y, Venditti RA, Rojas OJ. Reinforcing poly (ε-caprolactone) nanofibers with cellulose nanocrystals. *Appl Mater Interfaces*. 2009;1(9):1996–2004.
28. Duan K, Chen H, Huang J, et al. One-step synthesis of amino-reserved chitosan-graft-polycaprolactone as a promising substance of biomaterial. *Carbohydr Polym*. 2010;80(2):498–503.
29. Skotak M, Leonov AP, Larsen G, Noriega S, Subramanian A. Biocompatible and biodegradable ultrafine fibrillar scaffold materials for tissue engineering by facile grafting of L-lactide onto chitosan. *Biomacromolecules*. 2008;9(7):1902–1908.
30. Cui W, Li X, Zhou S, Weng J. Investigation on process parameters of electrospinning system through orthogonal experimental design. *J Appl Polym Sci*. 2007;103(5):3105–3112.
31. He W, Ma ZW, Yong T, Teo WE, Ramakrishna S. Fabrication of collagen-coated biodegradable polymer nanofiber mesh and its potential for endothelial cells growth. *Biomaterials*. 2005;26(36):7606–7615.
32. Gu P, Yang J, Wang J, Young MJ, Klassen H. Sequential changes in the gene expression profile of murine retinal progenitor cells during the induction of differentiation. *Mol Vis*. 2009;15:2111–2122.
33. Pfaffl MW. A new mathematical model for relative quantification in real-time RT–PCR. *Nucleic Acids Res*. 2001;29(9):e45.
34. Yu H, Wang W, Chen X, Deng C, Jing X. Synthesis and characterization of the biodegradable polycaprolactone-graft-chitosan amphiphilic copolymers. *Biopolymers*. 2006;83(3):233–242.
35. Deitzel JM, Kleinmeyer J, Harris D, Beck Tan NC. The effect of processing variables on the morphology of electrospun nanofibers and textiles. *Polymer*. 2001;42(1):261–272.
36. Jiang H, Fang D, Hsiao BS, Chu B, Chen W. Optimization and characterization of dextran membranes prepared by electrospinning. *Biomacromolecules*. 2004;5(2):326–333.
37. Gupta D, Venugopal J, Prabhakaran MP, et al. Aligned and random nanofibrous substrate for the in vitro culture of Schwann cells for neural tissue engineering. *Acta Biomater*. 2009;5(7):2560–2569.
38. Lee SJ, Lim GJ, Lee JW, Atala A, Yoo JJ. In vitro evaluation of a poly (lactide-co-glycolide)-collagen composite scaffold for bone regeneration. *Biomaterials*. 2006;27(18):3466–3472.
39. Zhu X, Cui W, Li X, Jin Y. Electrospun fibrous mats with high porosity as potential scaffolds for skin tissue engineering. *Biomacromolecules*. 2008;9(7):1795–1801.
40. Vaquette C, Babak VG, Baros F, et al. Zeta-potential and morphology of electrospun nano-and microfibers from biopolymers and their blends used as scaffolds in tissue engineering. *Mendeleev Commun*. 2008;18(1):38–41.
41. Zhu Y, Gao C, Liu X, Shen J. Surface modification of polycaprolactone membrane via aminolysis and biomacromolecule immobilization for promoting cytocompatibility of human endothelial cells. *Biomacromolecules*. 2002;3(6):1312–1319.